Polymer Bulletin (2022) 79:1751–1765
https://doi.org/10.1007/s00289-021-03587-z

ORIGINAL PAPER

Conventional and controlled radical polymerization redox-initiated by Cerium(IV) and Acrylamide as an intrinsically reducing inimer: a facile strategy to branched polyacrylamide

Yiwen Sun[1,2] · **Guangqun Zhai**[1,3]

Received: 10 September 2020 / Revised: 9 December 2020 / Accepted: 6 February 2021 /
Published online: 22 February 2021

Abstract

Since cerium(IV) ammonium nitrate (CAN) could oxidize amidyl N–H moieties into nitrogen-centered radicals under proper conditions to initiate radical polymerization, CAN-acrylamide (AAm) redox-initiated radical homo/co-polymerization in a conventional or controlled manner was exploited with AAm as an intrinsically reducing inimer. CAN oxidized AAm to initiate conventional radical homopolymerization at 50–60 °C, and viscosity-average molecular weight (MW) of polyacrylamide (PAAm) steadily increased with conversion because of the oxidation of amidyl N–H moieties of in-chain -AAm- units, but MW was in a range from 10^4 to 10^5. CAN-AAm redox-initiated radical co-polymerization of *N,N*-dimethylacrylamide (DMAAm) proceeded readily under optimized conditions and formed PAAm-co-PDMAAm with MW in a range from 10^5 to 10^6, and increasing simultaneously with conversion. CAN-AAm redox-initiated controlled radical homopolymerization was performed with $FeCl_3$ complexes as the deactivator, and the polymerization proceeded in a mechanism of reverse atom transfer radical polymerization (ATRP) and MW of PAAm increased in proportion to conversion. The PAAm chains contained a C–Cl terminal, which was confirmed by block co-polymerization with DMAAm via standard ATRP with PAAm as the macro-initiator.

Keywords Cerium(IV) ammonium nitrate · Acrylamide · *N,N*-Dimethylacrylamide · Conventional radical polymerization · Atom transfer radical polymerization

✉ Guangqun Zhai
zhai_gq@cczu.edu.cn

[1] Jiangsu Key Laboratory of Environmentally Friendly Polymeric Materials, School of Materials Science and Engineering, Changzhou University, Changzhou 213164, China

[2] Jiangsu Collaborative Innovation Centre of Photovoltaic Science and Engineering, Changzhou University, Changzhou 213164, Jiangsu, China

[3] National Experimental Demonstration Center for Materials Science and Engineering, Changzhou University, Changzhou 213164, P.R. China

Introduction

As the most technically important water-soluble polymers, AAm-based homopolymers and copolymers have been extensively utilized in a great variety of application. In general, AAm-based polymers are prepared by radical polymerization of acrylamide (AAm) initiated by proper redox-pairs under specific conditions to achieve tailor-designed structures and properties [1].

There have been several works on radical homopolymerization of AAm as both reducing initiator and monomer (i.e., intrinsically reducing inimer) with supervalent high-oxidation copper(III) complexes as the oxidizing agent [2, 3]. During the process, the copper(III) complexes oxidize the primary N–H moieties of AAm into amidyl nitrogen-centered radicals as the primary radicals via an electron-transfer followed by proton-transfer (ET-PT) process, which initiate the polymerization and gave rise to linear primary PAAm chains. The copper(III) complexes also oxidize the primary N–H moieties of in-chain -AAm- units into mid-chain amidyl nitrogen-centered macro-radicals to initiate graft polymerization. The molecular weight (MW) would grow gradually with the increasing conversion of AAm, and the polymerization leads to branched PAAm [2, 3]. However, most copper(III) complexes have to be prepared in situ and appear to be black, which renders it to rather difficult to visually monitor the polymerizations.

Cerium(IV) ammonium nitrate (CAN) complexes have also been reported to oxidize primary and secondary amidyl N–H moieties into amidyl nitrogen-centered radicals [4–6]. CAN could directly oxidize primary N–H moieties of AAm and initiate radical polymerization of AAm, yielding PAAm [7]. Thus, CAN-AAm forms a unique polymerizable redox-initiation pair in aqueous media with AAm as the intrinsically reducing inimer, leading to slightly branched polymers with in-chain -AAm- units as the branch sites. Each initiation by AAm leads to a linear primary linear chain, while each initiation by -AAm- units contributes to a graft side chain. In this work, with an objective to explore the potential of the CAN-AAm polymerizable redox-initiation pair in preparing branched PAAm, we examined CAN-AAm redox-initiated conventional radical homo/co-polymerization and reverse atom transfer radical polymerization (ATRP). Our results suggested that the CAN-AAm pair embraces great potentials in preparing branched polymers in aqueous solutions under mild conditions.

Experimental

Materials

N,N-Dimethylacrylamide (DMAAm, > 99.0%), from Volant Chemical Co. Ltd, Nantong, China, was purified by passing through a column fitted with Na_2CO_3, nanosilica and basic Al_2O_3 (from top to bottom) to remove inhibitors and then stored in a refrigerator before use. Other materials were used as

received. Acrylamide (AAm, ≥ 99.0%), 1,10-phenanthroline (Phen) and ascorbic acid (AA) were from Aladdin Biochemical Technology Co., Ltd, Shanghai, China. An aqueous stock solution of AAm ($[AAm]_0 = 5$ mol/L) was prepared in advance. $FeCl_3 \cdot 6H_2O$, NaCl and CAN were purchased from Shanghai Chemical Reagent Co. Ltd., Shanghai, China. Ethylenediaminetetraacetic acid tetrasodium salt (EDTA, > 99.0%) was from Shanfeng Chemical Co. Ltd, Changzhou, China. An aqueous stock solution of $FeCl_3 \cdot 6H_2O$ with different ligand ($[FeCl_3/ligand]_0 = 0.01$ mol/L) was prepared in advance. An aqueous stock solution of NaCl ($[NaCl]_0 = 0.10$ mol/L) was prepared in advance. An aqueous stock solution of CAN solution ($[CAN]_0 = 0.46$ mol/L, $[\text{nitric acid}]_0 = 1.0$ mol/L) was prepared in advance.

CAN-AAm Redox-initiated conventional radical polymerization of AAm

A predetermined volume of the stock solution of AAm and of CAN complexes, respectively, was added stepwise into the vessel. 1 mL DMF and a specific volume of deionized water were added to achieve a total volume at 50 mL. After degassing by a stream of high-purity Argon for 20 min, the solution was transferred into a water bath pre-set at 50 or 60 °C. Aliquots were collected at intervals and quenched by deionized water with MEHQ dissolved in advance. Conversion of AAm was estimated by gas chromatography with DMF as the internal standard. After aliquots were poured into copious ethanol, PAAm were precipitated, collected and dried in vacuo at 60 ℃ for 24 h. CAN-AAm redox-initiated conventional radical polymerization of DMAAm was conducted in a similar approach.

CAN-AAm redox-initiated reverse ATRP of AAm

A predetermined volume of the stock solutions of AAm, of Fe^{III}/ligand complexes, of NaCl and of CAN complexes, respectively, was added stepwise into the vessel. 1 mL DMF and a specific volume of deionized water were added to achieve a total volume at 50 mL. After degassing by a stream of high-purity Argon for 20 min, the solution was transferred into a water bath pre-set at 50℃. Aliquots were collected at intervals and quenched by deionized water with MEHQ dissolved in advance. Conversion of AAm was estimated by gas chromatography with DMF as the internal standard. After aliquots were poured into copious ethanol, PAAm were precipitated, collected and dried in vacuo at 60 ℃ for 24 h.

Preparation of PAAm-Cl as the macro-initiator and ATRP block polymerization

For the preparation of the macro-initiator (PAAm-Cl), 20 mL of the stock AAm solution, 3 mL of the stock solution of $FeCl_3$/EDTA:Phen complexes, 1 mL of the stock solution of CAN complexes, 0.3 mL of the stock solution of NaCl and 1 mL of DMF were added stepwise into the vessel. Deionized water was added to achieve a total volume at 50 mL. After degassing by a stream of high-purity of Argon for 20 min, the solution was transferred into a water bath pre-set at 50 °C. The mixture

was allowed to react for 4 h and quenched by exposure to air. After the reaction, ca. 25 mL of the viscous gel was collected to determine conversion of AAm and MW of the so-obtained PAAm-Cl.

For the ATRP chain extension with AAm, 50 mL of the stock AAm solution, 0.88 g of AA, 1 mL of DMF, 24 mL of deionized water were mixed with the second half of the above reacting solution to produce a homogenous solution. After degassing by a stream of high-purity Argon for 20 min, the solution was allowed to react at 80 °C for 6 h. After the polymerization, conversion of AAm was estimated by gas chromatography. After aliquots were poured into copious tetrafuran (THF), PAAm-b-PAAm were precipitated, collected and dried in vacuo at 60 ℃ for 24 h.

For the ATRP chain extension with DMAAm, 50 mL of DMAAm, 0.88 g of AA, 1 mL of DMF, 24 mL of deionized water were mixed with the second half of the above reacting solution to produce a homogenous solution. After degassing by a stream of high-purity Argon for 20 min, the solution was allowed to react at 80℃ for 6 h. After the polymerization, conversion of DMAAm was estimated by gas chromatography. After aliquots were poured into copious tetrafuran (THF), PAAm-b-PDMAAm were precipitated, collected and dried in vacuo at 60 ℃ for 24 h.

Characterization

Fourier-transformed infrared (FTIR) spectroscopy was performed on a Thermo-Fischer Nicolet-6700 FTIR spectroscope with KBr as the pellet matrix in the transmission mode (400–4000 cm^{-1}). GC was performed on a gas chromatograph (Kexiao GC-1690, Hangzhou, China) equipped with a capillary column (length: 30 m; internal diameter: 0.32 mm). The column temperature was elevated from 80 °C to 200 °C at a rate at 15 °C/min with high-purity nitrogen as the mobile phase at a rate of 30 mL/min. Conversion of AAm and DMAAm was estimated by calibration with DMF as the internal standard. MW of PAAm and PDMAAm was determined by using viscometry. PAAm was dissolved using aqueous NaCl solutions ($[NaCl]_0 = 0.5$ mol L^{-1}), and PDMAAm was dissolved using deionized H_2O as the solvent, with a concentration at 0.5–0.7 g/dL. The relative viscosity of the aqueous solutions of polymers was measured in a Ubbelohde-type viscometer thermally equilibrated in a SHP-501 super constant temperature bath (Hengping Scientific Instruments, Shanghai, China). The intrinsic viscosity ([η]) was fitted by the single point method using Eq. 1.

$$[\eta] = \frac{\sqrt{2\eta_{sp} - 2\ \ln}\ \eta_r}{c} \tag{1}$$

The measurement of the aqueous solution of PAAm was conducted at 25 °C and that of PDMAAm was carried out at 40 ℃. Their viscosity-average molecular weight (Mη) was estimated by using Mark–Houwink equation ($[\eta] = K \times M\eta^{\alpha}$; $K = 7.19 \times 10^{-3}$ mL g^{-1}, $\alpha = 0.77$ for PAAm; $K = 2.0 \times 10^{-2}$ mL g^{-1}, $\alpha = 0.65$ for PDMAAm) [8]. Proton nuclear magnetic resonance (^{1}H-NMR) spectroscopy was performed on a Bruker DMX 500 M NMR spectrometer in D_2O at room

temperature, and the data were treated using MestRec software and calibrated against tetramethylsilane.

Results and discussions

CAN-AAm redox-initiated conventional radical polymerization of AAm

The oxidation of amidyl N–H moieties by CAN into amidyl nitrogen-centered radicals has been reported since 1960s, and the polymerization of AAm initiated by CAN has been studied by Sato [4–7]. If they function in a similar fashion to copper(III) complexes, the CAN-AAm redox-initiated conventional radical homo/co-polymerization might proceed in a fashion as illustrated in Scheme 1.

Figure 1a shows the kinetic profiles of CAN-AAm redox-initiated conventional radical polymerization of AAm at 50 or 60℃ with an initial concentration of CAN ($[CAN]_0$) at 9.12×10^{-3} M. The polymerization occurred readily at 50 ℃. Conversion reached ca. 7% in 0.5 h and gradually increased to ca. 53% in 1 h. The polymerization appeared to cease when conversion reached ca. 63% in 2 h. The polymerization performed at 60 ℃ proceeded at a faster rate. Conversion reached ca. 42% in 0.5 h, 69% in 1 h and 90% in 5 h. Intrinsic viscosity ([η]) of the aqueous solution of PAAm was determined by single-point method using Solomon–Ciuta equation, which displays an error less than ± 4% at neutral media [8].

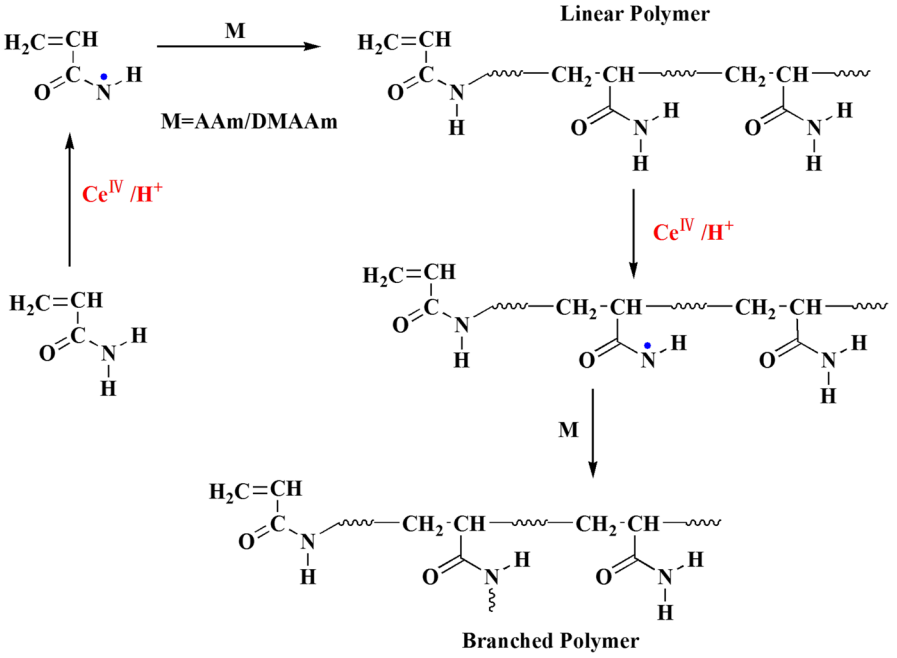

Scheme 1 CAN-AAm redox-initiated conventional radical homopolymerization and co-polymerization with DMAAm

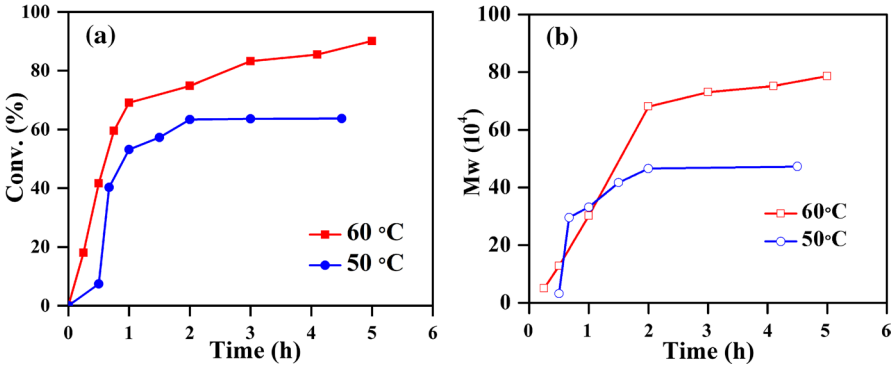

Fig. 1 **a** Conversion ~ Time Profiles of and **b** MW of PAAm formed as a function of reaction time during CAN-AAm Redox-initiated Conventional Radical Polymerization of AAm. Conditions: $[AAm]_0 = 4.0$ M, $[CAN]_0 = 9.12 \times 10^{-3}$ M, temperature = 50 ℃ or 60 ℃

Figure 1b compared MW of PAAm formed during the CAN-AAm redox-initiated conventional radical polymerization of AAm as a function of reaction time at 50 or 60 ℃. In common, MW of PAAm formed during the process grew gradually with the increasing conversion. For the process conducted at 50 ℃, MW of the PAAm increased from 3.14×10^4 in 0.5 h to 3.31×10^5 in 1 h and further to ca. 4.70×10^5 in 2 h. On the other hand, for the process conducted at 60 ℃, MW of the PAAm increased from 5.00×10^4 in 0.25 h, 3.01×10^5 in 1 h and further to ca. 6.81×10^5 in 2 h. Typical redox-initiated conventional radical polymerization of AAm in aqueous solutions without any chain transfer agents could easily generate PAAm with a MW above 10^6. Such a fact suggested that CAN might oxidize the PAAm propagating radicals into dead chains (oxidative elimination), similar to

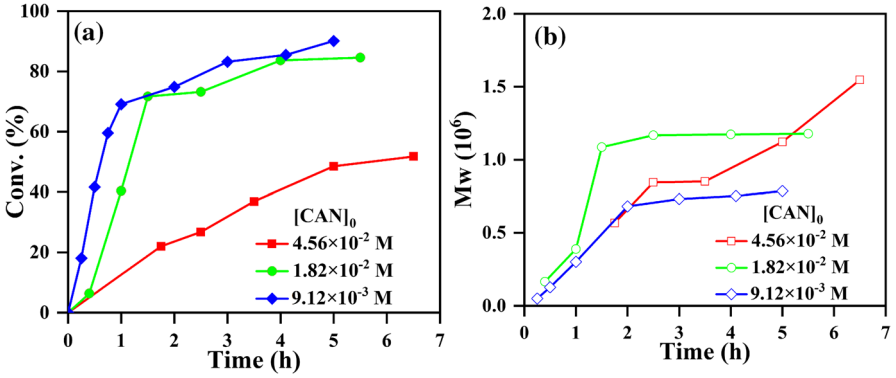

Fig. 2 **a** Conversion ~ Time Profiles of and **b** MW of PAAm formed as a function of reaction time during CAN-AAm Redox-initiated Conventional Radical Polymerization of AAm. Conditions: $[AAm]_0 = 4.0$ M, $[CAN]_0 = 9.12 \times 10^{-3}$, 1.82×10^{-2} and 4.56×10^{-2} M, temperature = 60 ℃

Cu^{III} complexes [2, 7]. It was implied that although CAN-AAm pairs could form a polymerizable redox initiator, such a technique cannot yield high-MW PAAm.

Figure 2a compares the kinetic profiles of CAN-AAm redox-initiated conventional radical polymerization of AAm at 60 ℃ with a different $[CAN]_0$. It was surprising to note that a higher concentration of CAN complexes exerted an adverse effect on the rate of polymerization, attributed to the oxidative elimination as stated earlier. On the other hand, Fig. 2b suggested that the concentration of CAN complexes exerted an adverse effect on the chain development of PAAm formed. In common, PAAm underwent further MW increase with the increasing conversion, but the polymerization with a higher $[CAN]_0$ corresponded to a more significant MW growth. Such a deviation was assigned to the stepwise oxidation of amidyl $–NH_2$ moieties of -AAm- units by CAN complexes into in-chain amidyl –N•H radicals, resulting in side chains, as also sketched in Scheme 1.

CAN-AAm redox-initiated conventional radical polymerization of DMAAm

CAN-AAm mono-centered polymerizable initiating pairs were used to initiate the radical polymerization of DMAAm. CAN cannot oxidize DMAAm to initiate polymerization in the absence of AAm under various conditions since no weak C-H or N–H moieties were present in DMAAm. Figure 3 shows the conversion ~ time profiles of CAN-AAm redox-initiated conventional radical polymerization of DMAAm with $[DMAAm]_0$ at 4.87 M and $[CAN]_0$ at 2.74×10^{-2} M. First, O_2 retarded the polymerization remarkably, as conversion reached 30% in 6.5 h under aerobic media, but conversion reached 91% in 5.1 h under deoxygenated media during the polymerization of DMAAm with $[AAm]_0$ at 0.30 M. Such retardation was negligible during the CAN-AAm redox-initiated conventional radical polymerization of AAm. Second, there was an optimum $[AAm]_0$ (0.30 M) at which the polymerization proceeded at the highest rate. Thus, $[AAm]_0$ was fixed at 0.30 M in the study.

Figure 4a shows the conversion ~ time profiles of CAN-AAm redox-initiated conventional radical polymerization of DMAAm with a $[CAN]_0$ at 1.34×10^{-2}, 1.82×10^{-2}, 2.74×10^{-2}, 3.65×10^{-2} and 4.56×10^{-2} M, respectively. When $[CAN]_0$

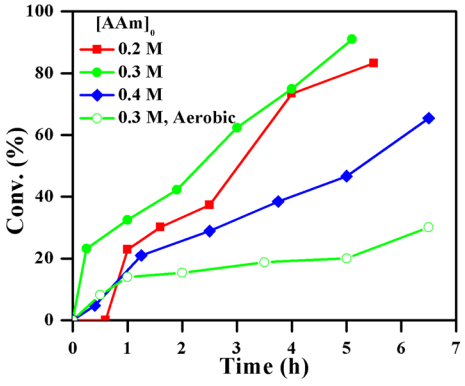

Fig. 3 Conversion ~ Time Profiles of CAN-AAm Redox-initiated Conventional Radical Polymerization of DMAAm. Conditions: $[AAm]_0 = 0.20$, 0.30 or 0.40 M, $[CAN]_0 = 2.74\times10^{-2}$ M, $[DMAAm]_0 = 4.87$ M, temperature = 60 ℃

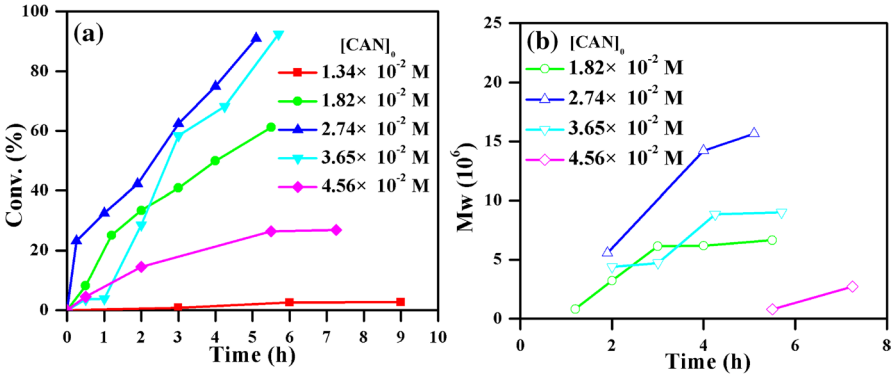

Fig. 4 **a** Conversion ~ Time Profiles of and **b** MW of PDMAAm formed as a function of reaction time during CAN-AAm Redox-initiated Conventional Radical Polymerization of DMAAm. Conditions: $[AAm]_0 = 0.30$ M; $[CAN]_0 = 1.34\times10^{-2}$, 1.82×10^{-2}, 2.74×10^{-2}, 3.65×10^{-2} and 4.56×10^{-2} M; $[DMAAm]_0 = 4.87$ M; temperature = 60 ℃

was below 2.74×10^{-2} M, the rate of polymerization could be enhanced by adding more CAN complexes. However, when $[CAN]_0$ was above 2.74×10^{-2} M, the rate of polymerization was further depressed with an increasing $[CAN]_0$, which was also assigned to the oxidation of the propagating radicals by CAN complexes. Figure 4b shows the MW of PDMAAm formed during the CAN-AAm redox-initiated conventional radical polymerization of DMAAm as a function of reaction time. When $[CAN]_0$ was below 2.74×10^{-2} M, no significant oxidative elimination occurred. As a result, not only the polymerization gave rise to high-MW PDMAAm, and increase in MW was observed with the further polymerization. For instances, during the polymerization with $[CAN]_0$ at 1.82×10^{-2} M, MW of PDMAAm increased from 8.14×10^5 in 1.2 h to 3.22×10^6 in 2 h and further to 6.66×10^6 in 5.5 h. During the polymerization with $[CAN]_0$ at 2.74×10^{-2} M, MW of PDMAAm increased from 5.56×10^6 in 1.9 h to 1.42×10^7 in 4 h and further to 1.56×10^7 in 5.1 h. It was implied that stepwise oxidation of amidyl $–NH_2$ moieties of -AAm- units by CAN complexes into in-chain amidyl –N•H radicals, resulting in side chains, contributed to the gradual MW growth of PDMAAm. Such a tendency would be compromised with a higher $[CAN]_0$. In particular, during the polymerization with $[CAN]_0$ at 4.56×10^{-2} M, MW of PDMAAm increased from 8.18×10^5 in 5.50 h to 2.73×10^6 in 7.0 h. Due to the low content of -AAm- units in PDMAAm, ^{1}H-NMR spectroscopy revealed that most units were -DMAAm- units, as shown in Fig. 5.

CAN-AAm redox-initiated reverse ATRP of AAm

Although CAN-AAm redox-initiated conventional homo/co-polymerization could be easily undertaken, several difficulties have to be taken into consideration to perform CAN-AAm redox-initiated reverse ATRP of AAm. CAN is a strong oxidizing agent, which could oxidize both organic substrates (alcohol, amides, amines, etc.) and transition-metal cation complexes in the low oxidation state (such as copper(I)

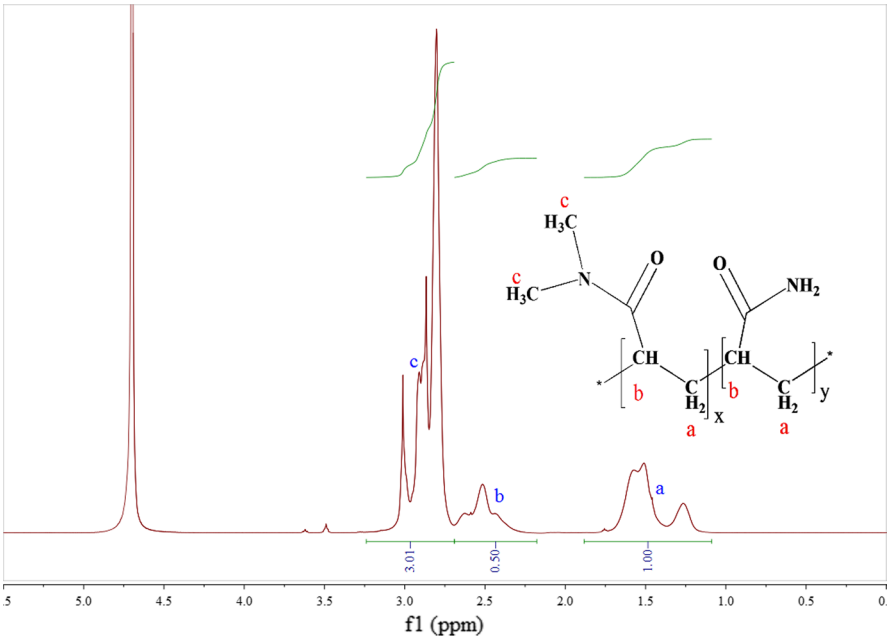

Fig. 5 ^{1}H-NMR spectrum of PAAm-co-PDMAAm in D_2O

and iron(II)). It was deemed that the rate constant of the latter process might be several orders of magnitude higher than the former one. Thus, Cu^{I} or Fe^{II} complexes cannot be used as the catalyst, otherwise most CAN would be consumed in oxidizing Cu^{I} or Fe^{II} complexes into Cu^{II} or Fe^{III} complexes. Correspondingly, the rate of primary initiation by CAN-amide pairs would be greatly depressed, as illustrated in Scheme 2a. Thus, Cu^{II} or Fe^{III} complexes could be used as the catalyst. It was

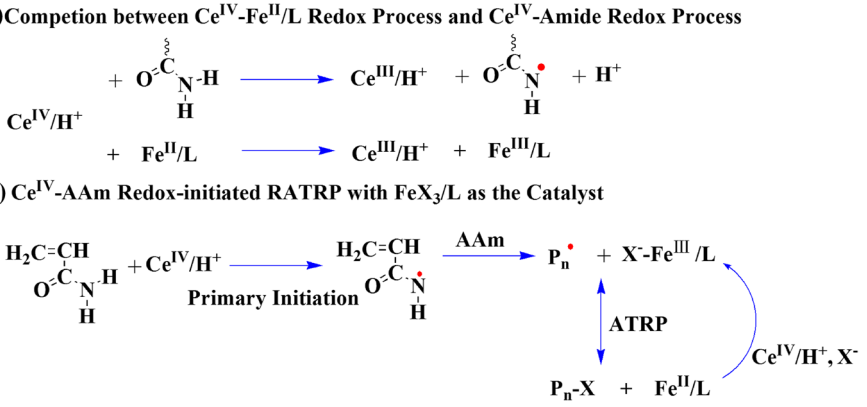

Scheme 2 **a** Competition between CAN-Amide redox process and CAN-FeII/L redox process; **b** Plausible CAN-AAm Redox-initiated reverse ATRP with FeX_3/L as the catalyst

assumed that the CAN-AAm redox-initiated reverse ATRP would proceed in a fashion outlined in Scheme 2b.

The brief screening on catalysts suggested that Cu^{II} complexes with typical di- or multi-dentate tertiary amine or pyridyl ligands failed to convey the controllability. It was attributed probably due to the nitric acid added to enhance the oxidizing potential of CAN. As the protonation of tertiary amine or pyridyl ligands by nitric acid would deteriorate their coordination with Cu^{II} complexes and thus fails to regulate their redox potential as ATRP catalysts, which renders direct ATRP of (meth) acrylic acid rather difficult for copper-based ATRP [9]. Such a challenge has been recently won by copper complexes with tris(2-pyridylmethyl)amine (TPMA) as the ligand with electrochemical mediation (eATRP) or Cu^0 as the supplemental activator and reducing agent (ATRP) [10, 11]. In comparison, iron-based ATRP appears to be more tolerant to acidic media (monomers [12], ligands [13] and additives [14]). There have been reports that $FeCl_3$ complexes with EDTA and Phen as the co-ligands (denoted as Fe^{III}/EDTA:Phen complexes) could mediate persulfate-initiated aqueous ATRP of AAm in a better-controlled fashion than those with Fe^{III}/EDTA or Fe^{III}/Phen complexes [15]. Thus, $FeCl_3$/EDTA:Phen complexes were used as the deactivator to catalyze the CAN-AAm redox-initiated reverse ATRP.

Since the oxidative termination of propagating radicals by CAN complexes was prominent at 60 °C, which led to ill-controlled behaviors, the polymerization was conducted at 50 ℃. Figure 6a compares the conversion ~ time profiles of CAN-AAm redox-initiated reverse ATRP at 50 ℃ with $[CAN]_0 = 9.12 \times 10^{-3}$ M, $[FeCl_3/EDTA:Phen]_0$ at 1.00×10^{-3} M and $[AAm]_0 = 2.0$, 3.0 and 4.0 M. In general, the polymerization displayed no dependence on the concentration of AAm. Figure 6b shows the MW of PAAm formed during CAN-AAm redox-initiated reverse ATRP as a function of conversion. It was obvious that MW of PAAm increased approximately in proportion to conversion, characteristic of the controlled radical polymerization and suggesting the constant concentration of PAAm chains throughout the processes. For the polymerization with $[AAm]_0$ at 3.0 M, MW of PAAm grew

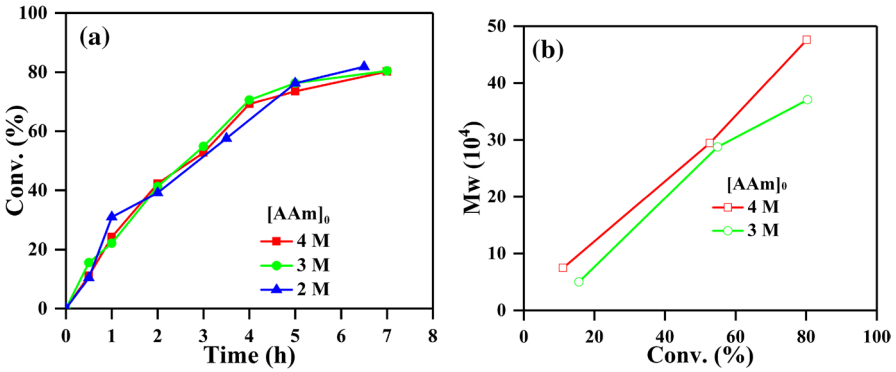

Fig. 6 **a** Conversion ~ Time Profiles of and **b** MW of PAAm formed as a function of conversion during CAN-AAm Redox-initiated Reverse ATRP at different $[AAm]_0$. Conditions: $[CAN]_0 = 9.12 \times 10^{-3}$ M, $[FeCl_3/EDTA:Phen]_0 = 1.00 \times 10^{-3}$ M, 50 ℃

from 5.00×10^4 at conversion 15.6% to 2.98×10^5 at conversion 54.9% and further to 3.70×10^5 at conversion 80.4%. For the polymerization with $[AAm]_0$ at 4.0 M, MW of PAAm grew from 7.45×10^4 at conversion 11.1% to 2.94×10^5 at conversion 52.7% and further to 4.76×10^5 at conversion 80.2%.

Figure 7a compares the conversion ~ time profiles of CAN-AAm redox-initiated reverse ATRP at 50℃ with $[CAN]_0$ at 9.12×10^{-3} M, $[AAm]_0$ at 2.0 M and various $[FeCl_3/EDTA:Phen]_0$. Within the concentration range, $FeCl_3$/EDTA:Phen complexes exhibited little effect on the rate of polymerization. Probably due to the high rate constant for propagation [15–20] and low rate constant for termination [16] of AAm in aqueous media, as well as hydrolytic instability of deactivating complexes (i.e., $(Fe^{III}\text{-}Cl^-)^{2+}$/EDTA:Phen complexes), the polymerization could still proceed during the process with $[FeCl_3/EDTA:Phen]_0$ slightly higher than $[CAN]_0$, but significant retardation was observed during the CAN-AAm redox-initiated reverse ATRP with $[FeCl_3/EDTA:Phen]_0$ at 2.00×10^{-3} M, as conversion reached merely 20% in 10 h, due to the efficient deactivation of propagating radicals by $FeCl_3$/EDTA:Phen complexes. If the reverse ATRP proceeds in a well-controlled fashion, the instantaneous concentration of propagating radicals should keep approximately constant. As a result, the semi-logarithmic plots ($\log([AAm]t/[AAm]_0)$ ~ time) would be in a straight line. However, in general, the semi-logarithmic plots derived from the processes suggested a moderately controlled behavior. In particular, the linear fitting indicated that the CAN-AAm redox-initiated reverse ATRP with $[FeCl_3/EDTA:Phen]_0$ at 6.00×10^{-4} M followed a first-order kinetics with a variance (R_2) at 0.96. Figure 7b shows the MW of PAAm formed during CAN-AAm redox-initiated reverse ATRP with $[FeCl_3/EDTA:Phen]_0$ at 6.00×10^{-4} M as a function of conversion. In general, the MW of PAAm grew simultaneously with the increasing conversion.

If the above process proceeded in well-controlled fashion of reverse ATRP, the sob-obtained PAAm should contain a C–Cl terminal group. Owed to the high MW of the so-obtained PAAm, it was difficult to identify the features from ^{1}H-NMR

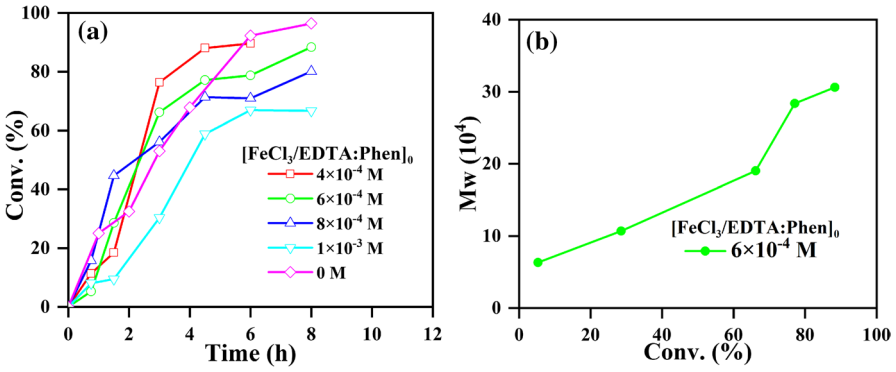

Fig. 7 **a** Conversion ~ Time Profiles of CAN-AAm Redox-initiated Reverse ATRP with different $[FeCl_3/EDTA:Phen]_0$ and **b** MW of PAAm formed as a function of conversion during CAN-AAm Redox-initiated Reverse ATRP at different $[FeCl_3/EDTA:Phen]_0$. Conditions: $[CAN]_0=9.12\times10^{-3}$ M, $[AAm]_0=2.0$ M, 50 ℃.

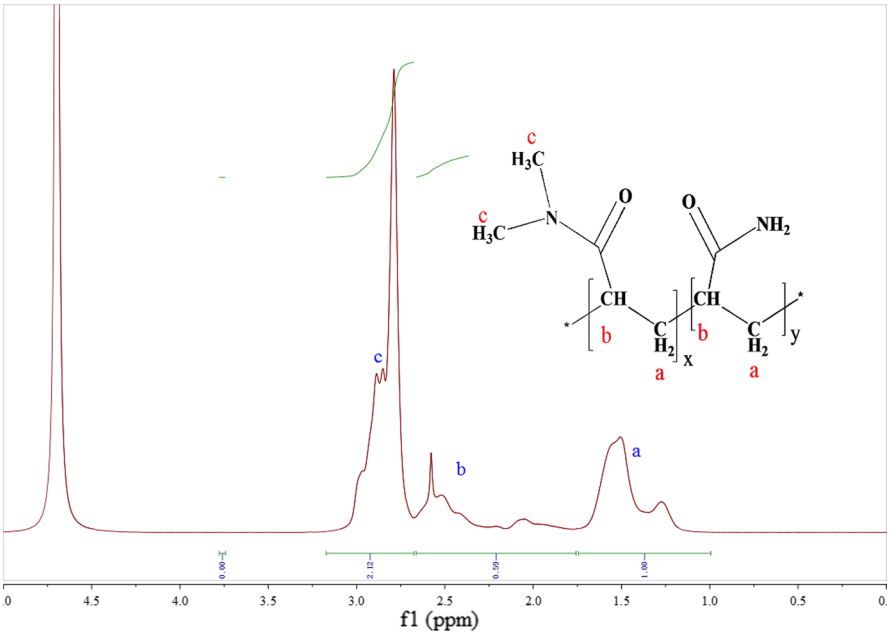

Fig. 8 ^{1}H-NMR spectrum of PAAm-block-PDMAAm in D_2O

spectrum. Therefore, we used the so-obtained PAAm (PAAm-Cl) as the macro-initiator to initiate polymerization of AAm and DMAAm via AGET ATRP with ascorbic acid (AA) as the reducing agent, during which, AA continuously in situ regenerated Fe^{III}/EDTA:Phen complexes into Fe^{II}/EDTA:Phen complexes as the activator

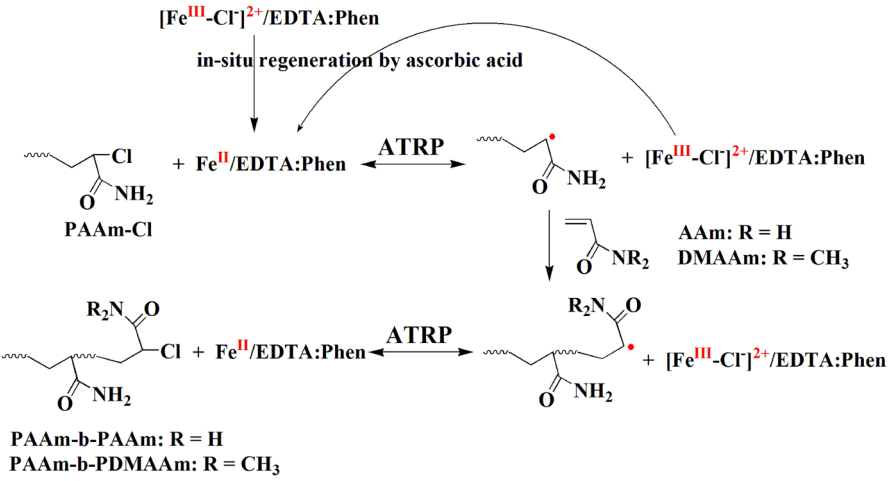

Scheme 3 $FeCl_3$/EDTA:Phen-catalyzed AGET ATRP of AAm or DMAAm with PAAm-Cl as the Macro-initiator and AA as the reducing agent

Table 1 Experimental Details of Reverse ATRP to prepare the Macro-initiator and MW of PAAm-Cl, PAAm-b-PAAm and PAAm-b-PDMAAm

Sample	CAN (mol/L)	$FeCl_3$/EDTA:Phen) (mol/L)	Conv. (%)	MW
PAAm-Cl	9.12×10^{-3}	6.0×10^{-4}	32	1.53×10^{5}
PAAm-b-PAAm	0	6.0×10^{-4}	22	4.52×10^{5}
PAAm-b-PDMAAm	0	6.0×10^{-4}	31	1.18×10^{6}

to catalyze ATRP initiated by PAAm-Cl. The process is outlined in Scheme 3. After the polymerization, MW of PAAm-b-PAAm and PAAm-b-PDMAAm was determined by viscometry and listed in Table 1. The polymerization occurred and led to polymer with a higher MW. Since CAN complexes have been depleted in preparing PAAm-Cl or oxidizing AA, the chain initiation during the block polymerization was exclusively initiated by PAAm-Cl. Thus, the CAN-AAm initiated radical polymerization in the presence of $FeCl_3$/EDTA:Phen complexes proceeded in a reverse ATRP mechanism and formed PAAm-b-PAAm and PAAm-b-PDMAAm.

Figure 8 shows the ^{1}H-NMR spectrum of PAAm-b-PDMAAm in D_2O. The peaks with a chemical shift (δ) in a range from 1.0 ppm to 1.75 ppm were attributed to the protons of in-chain methene (-CH_2-) moieties of both -AAm- units and -DMAAm- units. Those with δ from 1.75 ppm to 2.7 ppm were assigned to in-chain methine (-CH-) moieties of both -AAm- units and -DMAAm- units. The peaks with δ from 2.70 ppm to 3.2 ppm were associated with the pendant amidyl methyl (-$CON(CH_3)_2$) units of -DMAAm- units. The ^{1}H-NMR results suggested that -DMAAm- units took a predominant presence in the PAAm-b-PDMAAm, in a good agreement with the MW growth. Thus, it was implied that CAN-AAm redox-initiated radical polymerization in the presence of $FeCl_3$/EDTA:Phen proceeded in a reverse ATRP fashion and led to PAAm-Cl. On the other hand, the attempt to carry out CAN-AAm redo-initiated controlled radical polymerization of DMAAm with $FeCl_3$/EDTA:Phen complexes as the deactivator led to no success, which was attributed to much slow primary initiation in the presence of a much lower concentration of AAm.

Conclusion

CAN-AAm redox-initiated radical homo/co-polymerization in conventional or controlled manner was exploited with AAm as the intrinsically reducing inimer. CAN oxidized AAm to initiate conventional radical homopolymerization of AAm at 50–60℃, and MW of polyacrylamide (PAAm) steadily increased with the conversion, but MW was in a range from 10^4 to 10^5. CAN-AAm redox-initiated radical co-polymerization of DMAAm formed PAAm-co-PDMAAm with a MW from 10^5 to 10^6. CAN-AAm redox-initiated reverse ATRP was carried out in the presence of $FeCl_3$ complexes. MW of PAAm would increase in proportion to conversion and the PAAm contained a C–Cl terminal, confirming a mechanism of reverse ATRP.

Acknowledgement This work was supported by the Top-notch Academic Programs Project of Jiangsu Higher Education Institutions (TAPP) and the Priority Academic Program Development of Jiangsu Higher Education Institutions (PAPD).

References

1. Kulicke W-M, Kniewske R, Klein J (1982) Preparation, characterization, solution properties and rheological behaviour of polyacrylamide. Prog Polym Sci 8(4):373–468. https://doi.org/10.1016/0079-6700(82)90004-1
2. Liu Yh, Jb Li, Ly Y, Zq S (2003) Study on kinetics of acrylamide polymerization initiated by potassium ditelluratocuprate (III) in alkaline medium. J Macromol Sci Part A Pure Appl Chem 40(10):1107–1117. https://doi.org/10.1081/MA-120024465
3. Zhang X, Liu W, Chen Y, Gong A (1999) Self-condensing vinyl polymerization of acrylamide. Polym Bull 43:29–34. https://doi.org/10.1007/s002890050529
4. Haworth S, Holker JR (1966) Cerium–initiated polymerisation of some vinyl compounds in polyamide fibres. J Soc Dyers Colour 82(7):257–264. https://doi.org/10.1111/j.1478-4408.1966.tb02721.x
5. Pradhan AK, Pati NC, Nayak PL (1982) Grafting vinyl monomers onto nylon 6. V. Graft copolymerization of methyl methacrylate onto nylon 6 with the tetravalent cerium-thiourea redox system. J Polym Sci Part A: Polym Chem 20(1):257–261. https://doi.org/10.1002/pol.1982.170200130
6. Samal RK, Nayak MC, Panda G, Suryanarayana GV (1982) Polymerization of acrylonitrile. Kinetics of the reaction initiated by the Ce(IV)/thioacetamide redox system. J Polym Sci Part A: Polym Chem 20(1):53–62. https://doi.org/10.1002/pol.1982.170200106
7. Takahashi T, Hori Y, Sato I (1968) Coordinated radical polymerization and redox polymerization of acrylamide by ceric ammonium nitrate. J Polym Sci, Part A: Polym Chem 6(8):2091–2102. https://doi.org/10.1002/pol.1968.150060807
8. Curvale RA, Cesco JC (2019) Intrinsic viscosity determination by "single-point" and "double-point" equations. Appl Rheol 19(5):53347–1. https://doi.org/10.3933/ApplRheol-19-53347
9. Fantin M, Isse AA, Gennaro A, Matyjaszewski K (2015) Understanding the Fundamentals of Aqueous ATRP and Defining Conditions for Better Control. Macromolecules 48(19):6862–6875. https://doi.org/10.1021/acs.macromol.5b01454
10. Fantin M, Isse AA, Venzo A, Gennaro A, Matyjaszewski K (2016) Atom Transfer Radical Polymerization of Methacrylic Acid: A Won Challenge. J Am Chem Soc 138(23):7216–7219. https://doi.org/10.1021/jacs.6b01935
11. Lorandi F, Fantin M, Wang Y, Isse AA, Gennaro A, Matyjaszewski K (2020) Atom Transfer Radical Polymerization of Acrylic and Methacrylic Acids: preparation of Acidic Polymers with various architectures. ACS Macro Lett 9(5):693–699. https://doi.org/10.1021/acsmacrolett.0c00246
12. Fu L, Simakova A, Fantin M, WangOrcid Y, Matyjaszewski K (2018) Direct ATRP of Methacrylic Acid with Iron-Porphyrin based catalysts. ACS Macro Lett 7(1):26–30. https://doi.org/10.1021/acsmacrolett.7b00909
13. Xue Z, He D, Xie X (2015) Iron-catalyzed atom transfer radical polymerization. Polym Chem 6(10):1660–1687. https://doi.org/10.1039/C4PY01457J
14. Poli R, Allan LEN, Shaver MP (2014) Iron-mediated reversible deactivation controlled radical polymerization. Prog Polym Sci 39(10):1827–1845. https://doi.org/10.1016/j.progpolymsci.2014.06.003
15. Li L, Cao YF, Gu CJ, Liang LX (2009) Reverse atom transfer radical polymerization of acrylamide catalyzed by iron(III) system. J Dalian Polytech Univ 28(4):281–284. https://doi.org/10.3969/j.issn.1674-1404.2009.04.013
16. Giz A, Çatalgil-Giz H, Alb A, Brousseau J-L, Reed WF (2001) Kinetics and mechanisms of acrylamide polymerization from absolute, online monitoring of polymerization reaction. Macromolecules 34(5):1180–1191. https://doi.org/10.1021/ma000815s
17. Kurenkov VF, Myagchenkov VA (1980) Effects of Reaction Medium on the Radical Polymerization and Copolymerization of Acrylamide. Eur Polymer J 16(12):1229–1239. https://doi.org/10.1016/0014-3057(80)90030-0

18. Lacík I, Chovancová A, Uhelská L, Preusser C, Hutchinson RA, Buback M (2016) PLP-SEC Studies into the Propagation Rate Coefficient of Acrylamide Radical Polymerization in Aqueous Solution. Macromolecules 49(9):3244–3253. https://doi.org/10.1021/acs.macromol.6b00526
19. Pascal P, Napper DH, Gilbert RG, Piton MC, Winnik MA (1990) Pulsed laser study of the propagation kinetics of acrylamide and methacrylamide in water. Macromolecules 23(24):5161–5163. https://doi.org/10.1021/ma00226a024
20. Seabrook SA, Tonge MP, Gilbert RG (2005) Pulsed laser polymerization study of the propagation kinetics of acrylamide in water. J Polym Sci, Part A: Polym Chem 43(7):1357–1368. https://doi.org/10.1002/pola.20605